Electrical Detection of Metal Ions Using Field-Effect Transistors Based on Micropatterned Reduced Graphene Oxide Films

Herry Gunadi Sudibya,[†,⊥] Qiyuan He,[‡,⊥] Hua Zhang,[‡,§,*] and Peng Chen[†,*]

[†]School of Chemical and Biomedical Engineering, Nanyang Technological University, 70 Nanyang Drive, Singapore 637457, Singapore,
[‡]School of Materials Science and Engineering, Nanyang Technological University, 50 Nanyang Avenue, Singapore 639798, Singapore, and
[§]Centre for Biomimetic Sensor Science, Nanyang Technological University, 50 Nanyang Drive, Singapore 637553, Singapore

[⊥]These authors contributed equally to this work

ABSTRACT The electrical property of graphene is highly sensitive to its local environment, which makes graphene an ideal channel material in electronic sensors. Reduced graphene oxide (rGO) has been used as the desirable alternative to the pristine graphene due to its low-cost, solution-processable, and scalable production. In this paper, we present a field-effect transistor sensor using micropatterned, protein-functionalized rGO film as the conducting or sensing channel. Such a nanoelectronic sensor is able to detect various metal ions in real-time with high sensitivity.

KEYWORDS: reduced graphene oxide · field-effect transistors · metal ion detection · nanoelectronic detection

Graphene,[1] a two-dimensional and one-atom thick carbon sheet exhibiting exceptional electrical and physical properties, has received increasing attention due to its promising applications in electronics,[2] transparent electrodes,[3,4] and supercapacitors,[5] *etc.* More recently, graphene configured as field-effect transistors (FETs) has been employed as nanoelectronic biosensors for detection of biomolecules,[6,7] bacteria,[8] and cellular activities.[9,10] As compared to the one-dimensional semiconducting nanomaterials used for nanoelectronic biosensing,[11] graphene provides unique advantages due to its extremely high charge mobility and capacity,[2] large detection area, facile and homogeneous functionalization,[7] relatively low 1/*f* noise,[12] tunable ambipolar field-effect characteristics, and biocompatibility.[13] As all the charge carriers in graphene flow solely on the surface and expose directly to the sensing environment, the electrical property of graphene is highly sensitive to the minute electrochemical perturbations imposed by the biological targets or biological processes in solution.

Graphene can be obtained by mechanical or chemical exfoliation[1,14] or epitaxial growth on the SiC substrate.[15,16] Alternatively, graphene can be readily obtained by chemical reduction of graphene oxide.[17,18] Such a solution-based process allows the low-cost and large-scale production of graphene (more accurately, it is called reduced graphene oxide, rGO).[17,18] Recently, we have demonstrated that the long thin-film rGO micropatterns, generated by the microfluidics method, are able to electrically detect the dynamic secretion of hormone catecholamines from neuroendocrine PC12 cells.[10] Herein, we demonstrate a field-effect transistor (FET) sensor using protein-functionalized rGO films as the active channel for electronic detection of metal ions in aqueous solutions, which could be useful for the environmental analysis and biological applications. As compared to the often used fluorescence detection,[19,20] such a nanoelectronic sensor provides fast, real-time, simple, and label-free detection with high sensitivity.

RESULTS AND DISCUSSION

Figure 1A illustrates how to fabricate the reduced graphene oxide (rGO) micropatterns on 3-aminopropyltriethoxysilane (APTES)-modified quartz. The formed parallel rGO thin-film strips are 1 cm long, 10 μm wide, and 2−4 nm thick corresponding to 2−4 layers of rGO (AFM image in Figure 1A inset). After the drain and source electrodes were fabricated at both ends of the rGO patterns using conductive silver paste, the silicone rubber was used to insulate the two

* Address correspondence to chenpeng@ntu.edu.sg, hzhang@ntu.edu.sg.

Received for review November 9, 2010 and accepted February 9, 2011.

Published online February 21, 2011
10.1021/nn103043v

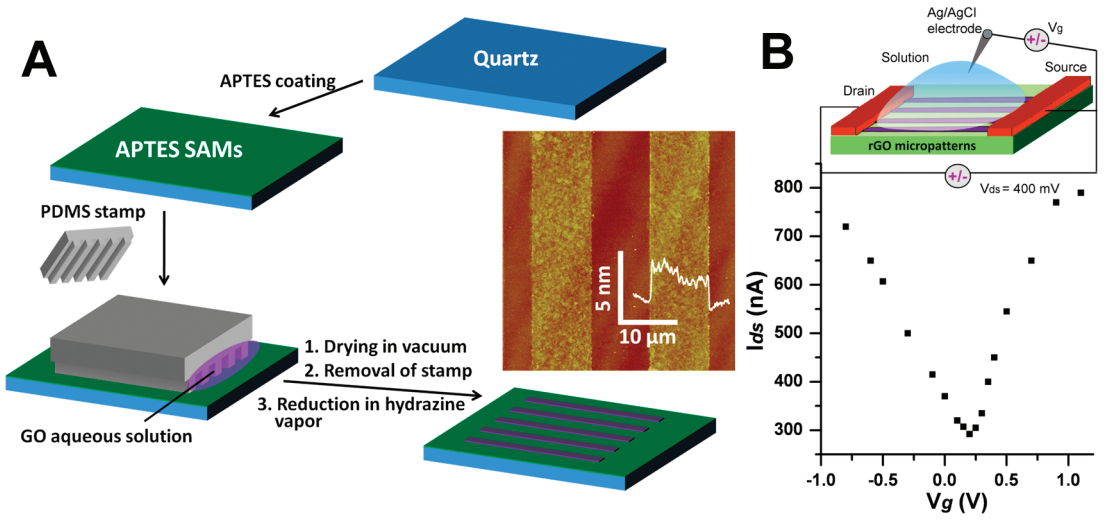

Figure 1. (A) Schematic illustration for fabrication of patterned rGO thin films on APTES-coated quartz. Inset: AFM image of the obtained rGO micropatterns on APTES-coated quartz. (B) Ambipolar characteristics of rGO-FET measured in 0.1× PBS buffer solution. Inset: Schematic of solution-gated configuration of rGO-FET.

electrodes and form the recording chamber. Figure 1B gives a typical plot of drain-to-source current (I_{ds}) *versus* solution-gate voltage (V_g) of our rGO based field-effect transistor (FET). Similar to the pristine graphene-based FET,[14] the ambipolar field-effect characteristics of our rGO-FET is evident, that is, the transition from p-type region to n-type region at the Dirac point of ~0.2 V.

The obtained patterned rGO FETs were used for detection of metal ions. We first explored the detection of Ca^{2+} ions, an important secondary messenger for cells and the major determinant for water hardness. To achieve specific detection, the rGO films were functionalized with calmodulin (CaM), a Ca^{2+} binding protein ubiquitously expressed in the eukaryotic cells, *via* the precoated pyrene linker molecules which covalently react with CaM in one end and firmly attach to rGO in the other end (pyrene tail) through the strong $\pi-\pi$ stacking interaction.[7]

In a typical experiment, as shown in Figure 2A (V_g = −0.6 V), the introduction of Ca^{2+} ions caused significant current (conductance) decrease in the CaM functionalized rGO-FET in a concentration-dependent manner. Both the p-type and n-type detection can be realized in the same rGO-FET by offsetting the solution-gate voltage (V_g). Figure 2B shows the statistics of device responses with different V_g values (−0.6, 0, and +0.6 V). In response to the addition of Ca^{2+} ions, the CaM-modified rGO-FETs exhibited the conductance decrease while operating at the p-type region (V_g = 0 or −0.6 V), and conductance increase while operating at the n-type region (V_g = +0.6 V). At V_g = −0.6 V, the detection limit of ~1 μM was achieved with a signal-to-noise ratio of ~20 to 30. This detection limit is consistent with the binding affinity (K_d) between Ca^{2+} and CaM, which is ~0.1 to 1 μM.[23,24] This detection limit is lower than that obtained by the silicon nanowire-based electronic sensor.[24] The detection of lower concentration could be achieved by functionalizing the rGO-FET sensors with a recognition element of higher binding affinity with Ca^{2+}, for example, silver hake parvalbumin with a binding affinity (K_d) of nM.[25]

CaM also binds to Mg^{2+}, but with much less affinity. Therefore, the rGO-FETs can also be used to detect Mg^{2+} (Figure 2C). As shown in Figure 2B and 2C, the change of conductance, caused by the binding of Ca^{2+} or Mg^{2+} onto rGO, can be attributed to the field-effect modulation of rGO-FETs introduced by the positively charged ions with the same sensing mechanism in the silicon nanowire-based Ca^{2+} sensors.[24] In contrast, the CaM-modified rGO-FETs did not show any response to the Na^+ and K^+ ions (Figure S1 in Supporting Information (SI)), indicating the specificity of detection due to the CaM functionalization of rGO. Furthermore, the rGO-FETs without functionalization of CaM are not sensitive to Ca^{2+} or Mg^{2+} (Figure S2 in SI), indicating that the CaM receptor is essential for the detection.

Furthermore, we explored the possibility for detection of heavy metals with our rGO-FETs. First, the metallothionein type II protein (MT-II), which binds with both physiological (*e.g.*, zinc, copper, selenium) and xenobiotic heavy (*e.g.*, cadmium, mercury) metals with high affinity, was functionalized onto the micropatterned rGO films *via* the pyrene linkers. As shown in Figure 3A, the addition of mercury (Hg^{2+}), at a concentration as low as 1 nM, caused the obvious current increase in the rGO-FET which was biased at V_{ds} = 400 mV and V_g = −0.6 V. As shown in Figure 3B, the magnitude of the device response scales with the Hg^{2+} concentration, and its polarity depends on the gate voltage (V_g). The detection limit for Hg^{2+} is about ~1 nM with a signal-to-noise ratio of 25−30.

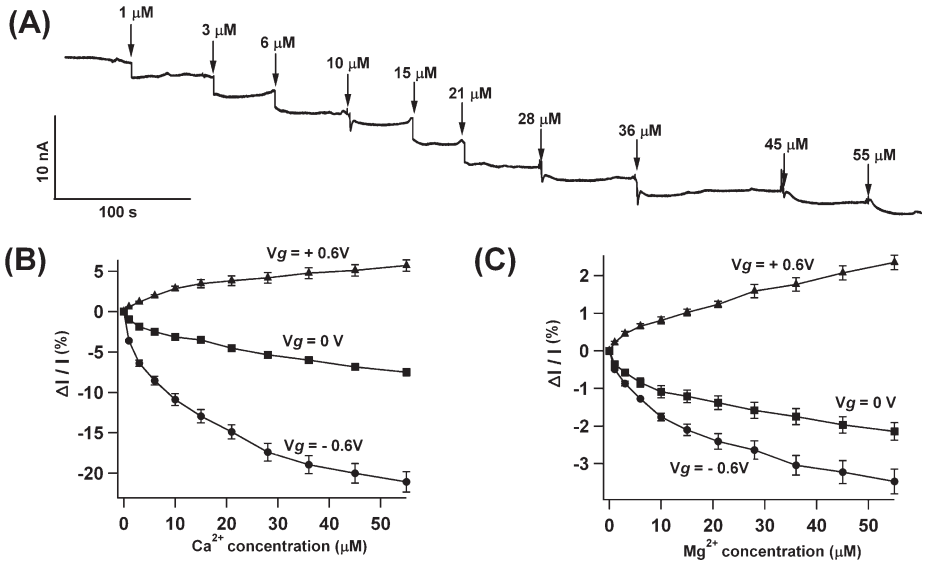

Figure 2. (A) Typical real-time recording of I_{ds} with the addition of Ca^{2+} ions. (B, C) The change of I_{ds} measured in rGO-FETs (tested sample number $n = 6$) with the addition of (B) Ca^{2+} and (C) Mg^{2+} ions at $V_{ds} = 0.4$ V and $V_g = -0.6$ (circle), 0 (square), and +0.6 V (triangle).

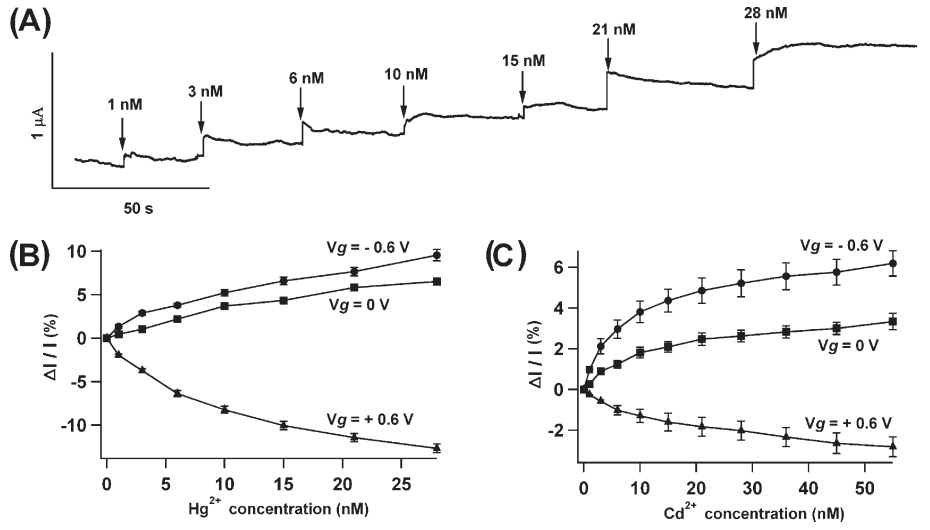

Figure 3. (A) Typical real-time recording of I_{ds} with the addition of Hg^{2+} ions. (B, C) The change of I_{ds} in rGO-FETs (tested sample number $n = 6$) with the addition of (B) Hg^{2+} and (C) Cd^{2+} ions at $V_{ds} = 0.4$ V and $V_g = -0.6$ (circle), 0 (square), and +0.6 V (triangle).

As compared to the detection of Ca^{2+}, the much higher sensitivity in Hg^{2+} detection arises from the high binding affinity of MT with the heavy metals (K_d in fM range).[26] To the best of our knowledge, this is the first demonstration of the real-time electronic detection of heavy metal ions based on our rGO-FET, which shows higher detection sensitivity than the previously reported fluorescence-based methods.[27−29] In addition, Cd^{2+} can also be detected at 1 nM with a slightly smaller change of current (signal-to-noise ratio of 15−20, Figure 3C).

It is noted that the polarity of device response caused by Hg^{2+} or Cd^{2+} is opposite to that of Ca^{2+} and Mg^{2+} (Figure 2B), although they all are positively charged. Therefore, the sensing mechanism of heavy metals does not arise from the field effect induced by the binding metal ions. It is known that binding of heavy metal ions causes a significant conformational change of MT.[26] Such conformational change might alter the interaction between the MT and rGO channel and consequently causes the conductance change in rGO-FETs. As MT-II (with an isoelectric point of 3.85) is highly negatively charged at neutral pH, it is conceivable that the conformation change upon metal binding brings MT-II closer to the rGO surface[26] and strengthens the field-effect imposed by the highly negatively charged MT-II. This is consistent to the observation that Hg^{2+} binding caused the positive-shift of the Dirac point of MT-functionalized rGO-FET (Supporting Information, Figure S3). Alternatively, the

rGO response may be explained by increased p-doping due to the stronger interaction between MT-II molecules and rGO upon metal ion binding. Further investigation is required to reveal the mechanism. In control experiments, we found that the MT-II modified rGO-FETs were not responsive to K^+, Na^+, Ca^{2+}, and Mg^{2+} (Supporting Information, Figure S4), and the rGO-FETs without functionalization with MT-II were not sensitive to Hg^{2+} and Cd^{2+} (Supporting Information, Figure S2).

The performance of our rGO sensors is stable. As shown in Supporting Information, Figure S5, a steplike current increase in response to Hg^{2+} remained constant during the long recording time (>15 min). The MT-II modified rGO-FETs can be reused for 3−4 times without any significant loss in the sensing sensitivity, after they are washed with acidic buffer (100 mM glycine, pH 2.3) to remove the bound metal ions from MT-II. Degradation of the devices performance was observed after over-reuse likely due to denaturation of the receptor proteins. To further demonstrate the practical use of our sensors, we tested the natural water collected from Nanyang Lake at our campus. As shown in the right inset of Figure 4, the addition of lake water, which is a complex soup consisting of various ions, microorganisms, and impurities, could not elicit any appreciable response of our devices. It indicates the high specificity of our sensors and proves that this small and isolated lake is not contaminated by heavy metals. In comparison, lake water with the addition of Hg^{2+} (concentration as low as 1 nM) caused a significant increase of rGO current while V_g was biased at −0.6 V (Figure 4). The experiments showed the practical use of our sensors in environmental monitoring.

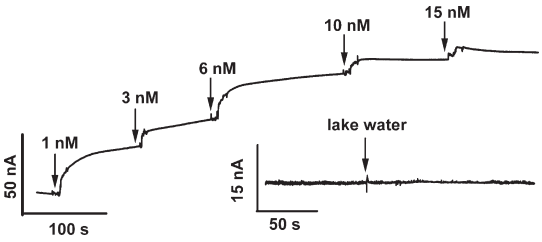

Figure 4. A typical real-time recording of I_{ds} with the addition of Hg^{2+} ions into 200 μL natural lake water on the top of rGO-FET device, with V_{ds} = 0.4 V and V_g = −0.6 V. Inset: Real-time recoding of I_{ds} with addition of 100 μL lake water into the existing 100 μL of DI water on the device.

CONCLUSION

Graphene and rGO based nanoelectronic devices are emerging as a new class of biosensors, promising a variety of biomedical applications. Here, we have demonstrated that a simple rGO-FET device readily fabricated on benchtop can be utilized to rapidly and label-freely detect various metal ions in solution with high sensitivity, specificity, and ease of use. This nanoelectronic approach is amenable for the development of lab-on-a-chip devices, and the array format of rGO patterns, in principle, enable parallel recording of multiple targets.

MATERIALS AND METHODS

Fabrication of Micropatterned Reduced Graphene Oxide Based Field-Effect Transistors. The micropatterned reduced graphene oxide (rGO) field-effect transistor (FET), referred to as rGO-FET, was fabricated based on our recently reported method (Figure 1A).[10] First, the homemade PDMS stamp with an array of line channels (10 μm width, 5 μm height, and 1.5 cm length) was treated with O_2 plasma to render the surface hydrophilic. Then it was pressed onto the 3-aminopropyltriethoxysilane (APTES)-modified quartz substrate[22] using a minitool (FX-117, Minitool Inc.) to ensure a firm contact. A drop of GO aqueous solution (*ca.* 1.5 mg/mL), synthesized by a modified Hummers method from the natural graphite,[21] was then dropped at one end of the open PDMS channels. The whole system was placed in a vacuum oven for 30 min to degas and dry up the solution. Subsequently, the PDMS stamp was carefully peeled off, leaving the GO micropatterns on the substrate. Parallel GO thin-film microstrips (1 cm long, 10 μm wide and 2−4 nm thick) were then chemically reduced in hydrazine vapor at 60 °C for 12 h[10,21] to obtain rGO film, followed by further thermal reduction/annealing at 600 °C in argon. Such thermal treatment improved the conductivity and stability of the devices, due to the further reduction of rGO film and enhancement of rGO-rGO stacking. After that, the drain and source electrodes were fabricated at both ends of rGO patterns using conductive silver paste. Finally, silicone rubber was used to insulate the electrodes and form the recording chamber. Each fabricated device contains 500 rGO strips.

Functionalization of Calmodulin (CaM) and Metallothionein (MT-II). The obtained rGO-FET was first incubated in 5 mM 1-pyrenebutanoic acid succinimidyl ester (i-DNA Biotechnology) in dimethylformaldehyde (DMF) at room temperature for 2 h, followed by rinsing with DI water and drying with N_2. It was then incubated in 1 mM buffer solution of calmodulin (CaM, Sigma) or metallothionein type II protein (MT-II), isolated from the rabbit liver (ITS Science and Medical), at 4 °C overnight, followed by a rinse with the phosphate buffer saline (PBS, pH 7.2).

Detection of Metal Ions. In the ion detection experiments, 200 μL of DI-water or Nanyang lake water was added into the recording chamber, in which an Ag/AgCl reference electrode was immersed in order to apply a desired gate voltage (V_g) (inset in Figure 1B). While the rGO-FET was biased at V_{ds} = 400 mV, the drain-to-source current (I_{ds}) was continuously monitored while the target ions were added to a defined concentration. Electrical measurements were carried out using a semiconductor device analyzer (Agilent, B1500A) with a sampling rate of 10 ms. The gate voltage was applied at −0.6, 0, or +0.6 V *via* the Ag/AgCl electrode immersed in the solution.

Acknowledgment. This work was supported by AcRF Tier 1 (RG 20/07) and AcRF Tier 2 (ARC 10/10, No. MOE2010-T2-1-060) from MOE, CRP (NRF-CRP2-2007-01) from NRF, A*STAR SERC Grants (No. 092 101 0064 and No. 072 101 0020) from A*STAR, New Initiative Fund FY 2010 (M58120031) from NTU, and the Centre for Biomimetic Sensor Science at NTU in Singapore. We

thank Shixin Wu for offering some GO sheets and Zongyou Yin for annealing some samples.

Supporting Information Available: Control experiments for ion detection with CaM functionalized rGO-FET, rGO-FETs, and MT-functionalized rGO-FET; $I_{ds}-V_g$ characteristics of MT-II-modified rGO-FET before and after addition of Hg^{2+}; long-time current stability in Hg^{2+} sensing with our rGO sensor. This material is available free of charge *via* the Internet at http://pubs.acs.org.

REFERENCES AND NOTES

1. Novoselov, K. S.; Geim, A. K.; Morozov, S. V.; Jiang, D.; Zhang, Y.; Dubonos, S. V.; Grigorieva, I. V.; Firsov, A. A. Electric Field Effect in Atomically Thin Carbon Films. *Science* **2004,** *306*, 666–669.
2. Geim, A. K.; Novoselov, K. S. The Rise of the Graphene. *Nat. Mater.* **2007,** *6*, 183–191.
3. Yin, Z. Y.; Sun, S.; Salim, T.; Wu, S. X.; Huang, X.; He, Q. Y.; Lam, Y. M.; Zhang, H. Organic Photovoltaic Devices Using Highly Flexible Reduced Graphene Oxide Films as Transparent Electrodes. *ACS Nano* **2010,** *4*, 5263–5268.
4. Yin, Z. Y.; Wu, S. X.; Zhou, X. Z.; Huang, X.; Zhang, Q. C.; Boey, F.; Zhang, H. Electrochemical Deposition of ZnO Nanorods on Transparent Reduced Graphene Oxide Electrodes for Hybrid Solar Cells. *Small* **2010,** *6*, 307–312.
5. Stoller, M. D.; Park, S. J.; Zhu, Y. W.; An, J. H.; Ruoff, R. S. Graphene-Based Ultracapacitors. *Nano Lett.* **2008,** *8*, 3498–3502.
6. Dong, X.; Shi, Y.; Huang, W.; Chen, P.; Li, L.-J. Electrical Detection of DNA Hybridization with Single-Base Specificity Using Transistors Based on CVD-Grown Graphene Sheets. *Adv. Mater.* **2010,** *22*, 1649–1653.
7. Huang, Y. X.; Dong, X. C.; Shi, Y. M.; Li, C. M.; Li, L. J.; Chen, P. Nanoelectronic Biosensors Based on CVD Grown Graphene. *Nanoscale* **2010,** *2*, 1485–1488.
8. Mohanty, N.; Berry, V. Graphene-Based Single-Bacterium Resolution Biodevice and DNA Transistor: Interfacing Graphene Derivatives with Nanoscale and Microscale Biocomponents. *Nano Lett.* **2008,** *8*, 4469–4476.
9. Cohen-Karni, T.; Qing, Q.; Li, Q.; Fang, Y.; Lieber, C. M. Graphene and Nanowire Transistors for Cellular Interfaces and Electrical Recording. *Nano Lett.* **2010,** *10*, 1098–1102.
10. He, Q. Y.; Sudibya, H. G.; Yin, Z. Y.; Wu, S. X.; Li, H.; Boey, F.; Huang, W.; Chen, P.; Zhang, H. Centimeter-Long and Large-Scale Micropatterns of Reduced Graphene Oxide Films: Fabrication and Sensing Applications. *ACS Nano* **2010,** *4*, 3201–3208.
11. Huang, Y. X.; Chen, P. Nanoelectronic Biosensing of Dynamic Cellular Activities Based on Nanostructured Materials. *Adv. Mater.* **2010,** *22*, 2818–2823.
12. Schedin, F.; Geim, A. K.; Morozov, S. V.; Hill, E. W.; Blake, P.; Katsnelson, M. I.; Novoselov, K. S. Detection of Individual Gas Molecules Adsorbed on Graphene. *Nat. Mater.* **2007,** *6*, 652–655.
13. Agarwal, S.; Zhou, X. Z.; Ye, F.; He, Q. Y.; Chen, G. C. K.; Soo, J.; Boey, F.; Zhang, H.; Chen, P. Interfacing Live Cells with Nanocarbon Substrates. *Langmuir* **2010,** *26*, 2244–2247.
14. Dong, X. C.; Shi, Y. M.; Zhao, Y.; Chen, D. M.; Ye, J.; Yao, Y. G.; Gao, F.; Ni, Z. H.; Yu, T.; Shen, Z. X.; *et al.* Symmetry Breaking of Graphene Monolayers by Molecular Decoration. *Phys. Rev. Lett.* **2009,** *102*, 135501.
15. Kim, K. S.; Zhao, Y.; Jang, H.; Lee, S. Y.; Kim, J. M.; Kim, K. S.; Ahn, J.-H.; Kim, P.; Choi, J.-Y.; Hong, B. H. Large-Scale Pattern Growth of Graphene Films for Stretchable Transparent Electrodes. *Nature* **2009,** *457*, 706–710.
16. Berger, C.; Song, Z. M.; Li, X. B.; Wu, X. S.; Brown, N.; Naud, C.; Mayou, D.; Li, T. B.; Hass, J.; Marchenkov, A. N.; *et al.* Electronic Confinement and Coherence in Patterned Epitaxial Graphene. *Science* **2006,** *312*, 1191–1196.
17. Dong, X. C.; Su, C. Y.; Zhang, W. J.; Zhao, J. W.; Ling, Q. D.; Huang, W.; Chen, P.; Li, L. J. Ultralarge Single-Layer Graphene Obtained from Solution Chemical Reduction and Its Electrical Properties. *Phys. Chem. Chem. Phys.* **2010,** *12*, 2164–2169.
18. Tung, V. C.; Allen, M. J.; Yang, Y.; Kaner, R. B. High-Throughput Solution Processing of Large-Scale Graphene. *Nat. Nanotechnol.* **2009,** *4*, 25–29.
19. Wanichacheva, N.; Watpathomsub, S.; Lee, V. S.; Grudpan, K. Synthesis of a Novel Fluorescent Sensor Bearing Dansyl Fluorophores for the Highly Selective Detection of Mercury (II) Ions. *Molecules* **2010,** *15*, 1798–1810.
20. Wang, E. J.; Ma, L.; Zhu, L.; Stivanello, C. M. Calcium Optical Sensors Based on Lipophilic Anionic Dye and Calcium-Selective Organophosphate Ionophore or Neutral Carrier. *Anal. Lett.* **1997,** *30*, 33–44.
21. Zhou, X. Z.; Huang, X.; Qi, X. Y.; Wu, S. X.; Xue, C.; Boey, F. Y. C.; Yan, Q. Y.; Chen, P.; Zhang, H. *In Situ* Synthesis of Metal Nanoparticles on Single-Layer Graphene Oxide and Reduced Graphene Oxide Surfaces. *J. Phys. Chem. C* **2009,** *113*, 10842–10846.
22. Li, H.; Zhang, J.; Zhou, X.; Lu, G.; Yin, Z.; Li, G.; Wu, T.; Boey, F.; Venkatraman, S. S.; Zhang, H. Amino Silane Micropatterns on Hydroxyl-Terminated Substrates: Fabrication and Applications. *Langmuir* **2010,** *26*, 5603–5609.
23. Klee, C. B.; Vanaman, T. C. *Calmodulin in Advances in Protein Chemistry*; Academic Press: 1982, 35, 213−321.
24. Cui, Y.; Wei, Q.; Park, H.; Lieber, C. M. Nanowire Nanosensors for Highly Sensitive and Selective Detection of Biological and Chemical Species. *Science* **2001,** *293*, 1289–1292.
25. Haiech, J.; Derancourt, J.; Pechere, J. F.; Demaille, J. G. Magnesium and calcium binding to parvalbumins: evidence for differences between parvalbumins and an explanation of their relaxing function. *Biochemistry* **1979,** *18*, 2752–2758.
26. Bontidean, I.; Berggren, C.; Johansson, G.; Csöregi, E.; Mattiasson, B.; Lloyd, J. R.; Jakeman, K. J.; Brown, N. L. Detection of Heavy Metal Ions at Femtomolar Levels Using Protein-Based Biosensors. *Anal. Chem.* **1998,** *70*, 4162–4169.
27. Nolan, E. M.; Lippard, S. J. Turn-On and Ratiometric Mercury Sensing in Water with a Red-Emitting Probe. *J. Am. Chem. Soc.* **2007,** *129*, 5910–5918.
28. Liu, X.; Tang, Y.; Wang, L.; Zhang, J.; Song, S.; Fan, C.; Wang, S. Optical Detection of Mercury(II) in Aqueous Solutions by Using Conjugated Polymers and Label-free Oligonucleotides. *Adv. Mater.* **2007,** *19*, 1471–1474.
29. Li, J.; Meng, J.; Huang, X. B.; Cheng, Y. X.; Zhu, C. J. A Highly Selective Fluorescent Sensor for Hg^{2+} Based on the Water-Soluble Poly(*p*-phenyleneethynylene). *Polymer* **2010,** *51*, 3425–3430.